Article

Molecular Cell

RNA Circularization Diminishes Immunogenicity and Can Extend Translation Duration *In Vivo*

Graphical Abstract

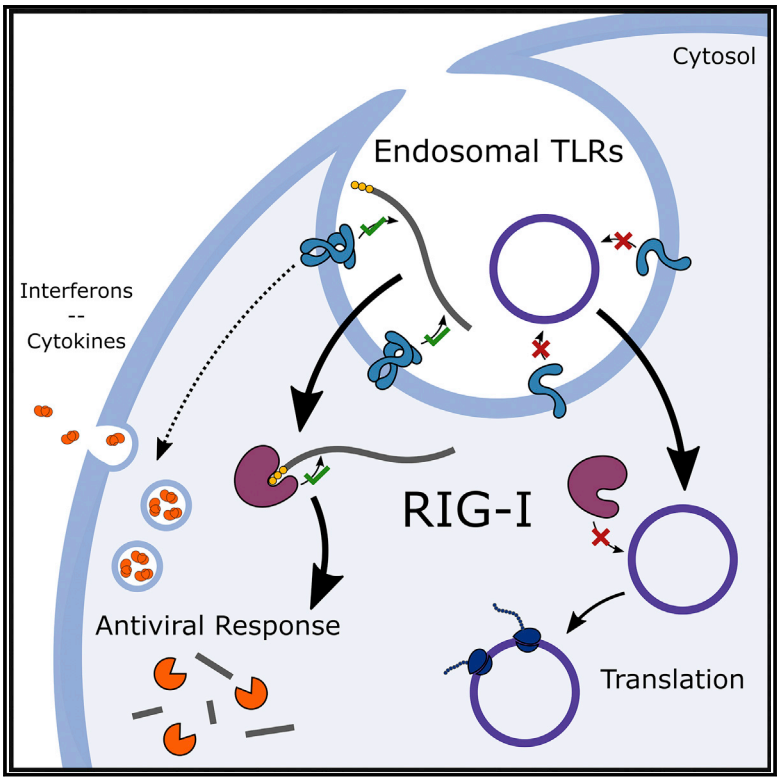

Authors

R. Alexander Wesselhoeft,
Piotr S. Kowalski,
Frances C. Parker-Hale,
Yuxuan Huang, Namita Bisaria,
Daniel G. Anderson

Correspondence

dgander@mit.edu

In Brief

Wesselhoeft et al. find that exogenous circular RNAs are able to bypass RNA sensors, thereby avoiding antiviral defense induction upon cellular entry. They report that nanoformulated, synthetic protein-coding circRNA can be translated in mouse tissues, providing evidence for the potential of circRNA as a vector for therapeutic gene expression.

Highlights

- Triphosphorylated and linear RNA contaminants provoke innate immune responses
- Purified exogenous circRNA does not trigger RIG-I
- circRNA does not trigger TLRs in overexpression cell lines
- Nanoformulated circRNA is translated in mouse tissues

Wesselhoeft et al., 2019, Molecular Cell *74*, 508–520
May 2, 2019
https://doi.org/10.1016/j.molcel.2019.02.015

CellPress

CellPress

Molecular Cell
Article

RNA Circularization Diminishes Immunogenicity and Can Extend Translation Duration *In Vivo*

R. Alexander Wesselhoeft,[1,2] Piotr S. Kowalski,[1,3] Frances C. Parker-Hale,[2,4] Yuxuan Huang,[1] Namita Bisaria,[5] and Daniel G. Anderson[1,3,6,7,8,*]

[1]David H. Koch Institute for Integrative Cancer Research, Massachusetts Institute of Technology, Cambridge, MA 02142, USA
[2]Department of Biology, Massachusetts Institute of Technology, Cambridge, MA 02142, USA
[3]Department of Chemical Engineering, Massachusetts Institute of Technology, Cambridge, MA 02142, USA
[4]Department of Political Science, Massachusetts Institute of Technology, Cambridge, MA 02142, USA
[5]Whitehead Institute for Biomedical Research, Cambridge, MA 02142, USA
[6]Institute for Medical Engineering and Science, Massachusetts Institute of Technology, Cambridge, MA 02142, USA
[7]Harvard and MIT Division of Health Science and Technology, Massachusetts Institute of Technology, Cambridge, MA 02142, USA
[8]Lead Contact
*Correspondence: dgander@mit.edu
https://doi.org/10.1016/j.molcel.2019.02.015

SUMMARY

Circular RNAs (circRNAs) are a class of single-stranded RNAs with a contiguous structure that have enhanced stability and a lack of end motifs necessary for interaction with various cellular proteins. Here, we show that unmodified exogenous circRNA is able to bypass cellular RNA sensors and thereby avoid provoking an immune response in RIG-I and Toll-like receptor (TLR) competent cells and in mice. The immunogenicity and protein expression stability of circRNA preparations are found to be dependent on purity, with small amounts of contaminating linear RNA leading to robust cellular immune responses. Unmodified circRNA is less immunogenic than unmodified linear mRNA *in vitro*, in part due to the evasion of TLR sensing. Finally, we provide the first demonstration to our knowledge of exogenous circRNA delivery and translation *in vivo*, and we show that circRNA translation is extended in adipose tissue in comparison to unmodified and uridine-modified linear mRNAs.

INTRODUCTION

Circular RNAs (circRNAs) are a class of RNAs with a range of protein-coding and non-coding functions (Legnini et al., 2017; Li et al., 2015; Hansen et al., 2013; Barrett and Salzman, 2016). Eukaryotic cells generate circRNAs through backsplicing (Chen and Yang, 2015; Jeck and Sharpless, 2014; Wang and Wang, 2015), while the genomes of viral pathogens such as hepatitis D virus and plant viroids can also be circular (Sanger et al., 1976; Kos et al., 1986). It has recently been proposed that cells have evolved a splicing-dependent mechanism for the discrimination of endogenous and exogenous circRNA, using RIG-I as a cytoplasmic sensor of exogenous circRNA (Chen et al., 2017; Loo and Gale, 2011). While circRNA does not contain the triphosphate motif canonically required for RIG-I activation, it has been suggested that RIG-I may transiently interact with circRNA that is devoid of host nuclear proteins, leading to a typical RIG-I mediated antiviral response (Chen et al., 2017). However, the mechanism of RIG-I-mediated recognition of circRNA remains unclear. In addition to RIG-I, it is also possible that circRNA interacts with other RNA sensors such as the endosomal Toll-like receptors (TLRs) 3, 7, and 8, which have been shown to activate signaling in response to linear single-stranded RNA (ssRNA) and double-stranded RNA (dsRNA) structures, as well as RNA degradation products such as uridine and guanosine-uridine-rich fragments (Tanji et al., 2015; Tatematsu et al., 2013; Bell et al., 2006; Zhang et al., 2016). To reduce an innate cellular immune response to exogenous RNA, nucleoside modifications such as pseudouridine (ψ), N^1-methylpseudouridine (m1ψ), and 5-methoxyuridine (5moU) have been developed for use in linear mRNA (Karikó et al., 2008, 2011; Svitkin et al., 2017). These modifications have been shown to prevent linear mRNA from activating TLRs and RIG-I (Karikó et al., 2005; Durbin et al., 2016). RNA modification with N^6-methyladenosine (m6A) has been shown to mediate cap-independent translation in endogenous linear and circRNAs (Meyer et al., 2015; Yang et al., 2017). To our knowledge, the contribution of TLRs to circRNA immunogenicity and the effects of nucleoside modifications, including m1ψ and m6A on exogenous circRNA translation, stability, and immunogenicity, have yet to be reported.

Recently, circRNA was developed for stable protein production in mammalian cells (Wesselhoeft et al., 2018). We sought to investigate the immunogenicity and translatability of exogenous circRNA *in vitro* and *in vivo* to determine the potential utility of circRNA for protein production applications. Here, we demonstrate that exogenous circRNA does not stimulate a cellular immune response in RIG-I and TLR competent cells. In addition, we show that unlike linear mRNA, circRNA does not benefit from modification with m1ψ in terms of protein expression and immunogenicity or from modification with m6A in terms of protein expression. We also find that circRNA is compatible with lipid nanoparticle-mediated delivery and is effectively translated

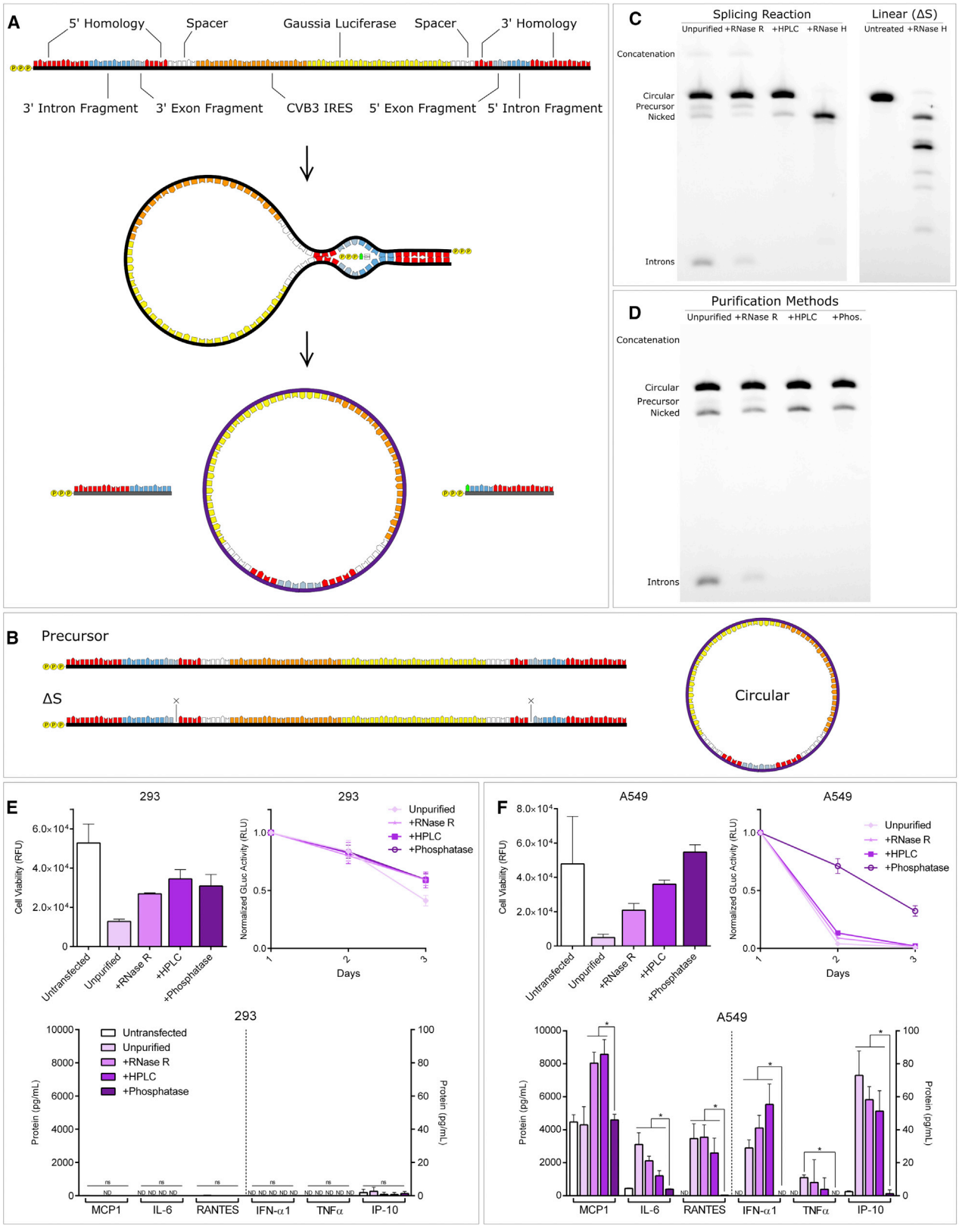

(legend on next page)

in vivo without provoking an RNA-mediated innate immune response, while protein expression from circRNA exhibits greater stability than that from uridine-modified linear mRNA in adipose tissue.

RESULTS

Purification of Exogenous circRNA Ablates Immunogenicity

Using the optimized permuted intron-exon (PIE) splicing method previously reported (Wesselhoeft et al., 2018), we synthesized circRNA precursors containing a coxsackievirus B3 internal ribosome entry site (CVB3 IRES), a Gaussia luciferase (GLuc) message, two designed spacer sequences, two short regions corresponding to exon fragments of the PIE construct, and the 3′ and 5′ intron segments of the permuted Anabaena pre-tRNA group I intron (Puttaraju and Been, 1992) by run-off transcription (Figures 1A and 1B; Table S1). In the presence of guanosine triphosphate (GTP) and Mg^{2+}, these precursor RNA molecules undergo the double transesterification reactions that are characteristic of group I catalytic introns, but because the exons are already fused, the region between the two intron segments is excised as a covalently 5′ to 3′ linked circle (Puttaraju and Been, 1992) (Figure 1A). To confirm that we obtained circular products, we treated the splicing reaction with RNase R, a 3′ to 5′ RNA exonuclease (Suzuki et al., 2006), and observed the enrichment of the putative circRNA band (Figure 1C). Subsequent purification of the RNase R-treated splicing reaction by high-performance liquid chromatography (HPLC) and then digestion with oligonucleotide-targeted RNase H produced a single major band in contrast to two major bands yielded by RNase H-digested linear precursor RNA that contains all of the same sequence elements as the circRNA precursor, with the exception of the splice site (ΔS) nucleotides (Figure 1C), confirming circularity. Splicing reactions containing circRNA demonstrated improved protein expression and expression stability in comparison to polyadenylated and phosphatase-treated linear precursors after transfection into 293 cells (Figures S1A–S1C).

To probe the immunogenicity of circRNA, we selected two cell lines (human embryonic kidney, 293; human lung carcinoma, A549) that we observed to elicit differential cell viability and GLuc expression stability responses upon transfection of unpurified circRNA splicing reactions (Figures 1E, 1F, and S2B). After the circularization protocol, these splicing reactions are expected to contain circRNA, excised triphosphorylated introns, linear and circular concatenations, and degradation products of both linear RNA and circRNA, some of which is triphosphorylated. While the splicing reaction proceeds nearly to completion under the circularization conditions we used, some triphosphorylated linear precursor RNA is also present. We therefore applied additional steps of purification to the unpurified splicing reactions and confirmed circRNA enrichment by gel electrophoresis: RNase R to enrich circRNA, HPLC to remove non-circular components, and phosphatase to remove residual triphosphates (Figure 1D). To determine the extent of the innate cellular immune response to transfected RNA, we monitored the release of a wide range of cytokines and chemokines into the culture medium, as well as the stability of protein expression from circRNA and cell viability.

We found that RNase R digestion of splicing reactions was insufficient to prevent cytokine release in A549 cells in comparison to untransfected controls (Figures 1F and S1D). The addition of HPLC purification was furthermore insufficient to prevent cytokine release, although we did note a significant reduction in interleukin-6 (IL-6) and a significant increase in interferon-α1 (IFN-α1) compared to the unpurified splicing reaction, suggesting that combined RNase R and HPLC may have depleted some immunogenic RNA species while enriching others (Figure 1F). The addition of a phosphatase treatment after HPLC purification and before RNase R digestion dramatically reduced the expression of all upregulated cytokines that we assessed in A549 cells, with secreted monocyte chemoattractant protein 1 (MCP1), IL-6, IFN-α1, tumor necrosis factor α (TNF-α), and IFN-γ inducible protein-10 (IP-10) falling to undetectable or untransfected baseline levels (Figure 1F). We did not observe a substantial cytokine release in 293 cells, consistent with our observation that the 3-day protein expression stability phenotype of these cells is relatively unaffected by the degree of circRNA purity and previous reports indicating that 293 cells do not express several key RNA sensors (Figures 1E and S1D) (Hornung et al., 2002). In contrast, increased circRNA purity improved GLuc expression stability in transfected A549 cells, with completely purified circRNA demonstrating a stability phenotype similar to that of transfected 293 cells (Figures 1E and 1F). Likewise, a trend of increased circRNA purity improved A549 cell viability 3 days post-transfection, while

Figure 1. Design, Synthesis, and Purification of circRNA

(A) Precursor RNA design and self-splicing overview. Colors denote different regions of the RNAs used in this article.

(B) Schematics of RNAs introduced and used in this figure. ΔSplice Sites (ΔS) are identical to the precursor RNA, except for small deletions encompassing both splice sites.

(C) Agarose gel showing precursor RNA after splicing, RNase R digestion, HPLC purification, and oligonucleotide-guided RNase H digestion. Circular RNA is digested by RNase H into one major band, while ΔS is digested into two major bands, confirming circularity.

(D) Agarose gel showing cumulative purification methods applied to circRNA. +RNase R, unpurified circRNA digested with RNase R only; +HPLC, unpurified circRNA HPLC purified, and then digested with RNase R; +Phos, unpurified circRNA HPLC purified, treated with a phosphatase, and then digested with RNase R.

(E) Cell viability, GLuc expression stability, and cytokine release from 293 cells transfected with different circRNA preparations, as described in (D). Cell viability was assessed 3 days after transfection. Cytokine release was assessed 24 h after transfection (data presented as means + SDs; n = 3; ns = not significant; *p < 0.05; ND, not detected).

(F) Cell viability, circRNA expression stability, and cytokine release from A549 cells transfected with different circRNA preparations, as described in (D). Cell viability was assessed 3 days after transfection. Cytokine release was assessed 24 h after transfection (data presented as means + SDs; n = 3; *p < 0.05; ND, not detected).

See also Figure S1.

293 cell viabilities remained largely unaffected, which is consistent with a lack of inflammatory signaling in 293 cells and diminishing inflammatory signaling in A549 cells with increasing circRNA purity (Figures 1E and 1F). Intact ^{32}P-labeled circRNA was present 6 and 24 h after transfection into 293 or A549 cells (Figures S1E and S1F). These results demonstrate that circRNA purity strongly affects its immunogenic potential and that fully purified circRNA is significantly less immunogenic than unpurified or incompletely purified splicing reactions. The stability of protein expression from circRNA is also dependent on circRNA purity and the sensitivity of transfected cell types to contaminating RNA species.

Non-circular Components of the Splicing Reaction Contribute to Immunogenicity

To explore the source of immunogenicity in circRNA splicing reactions, we purified each component of the splicing reaction by HPLC and assessed cytokine release and cell viability upon transfection of A549 cells (Figures 2A and 2B). Because we had difficulty obtaining suitably pure linear precursor RNA from the splicing reaction, we separately synthesized and purified precursor RNA in the form of the splice site deletion mutant (ΔS) (Figure 2B, bottom right). In addition, we split the circRNA peak into two fractions to control for nicked RNA peak overlap (Figure 2B). We observed robust IL-6, RANTES, and IP-10 release in response to most of the species present within the splicing reaction, as well as precursor RNA (Figures 2C, S2A, and S2C). Early circRNA fractions elicited cytokine responses comparable to other non-circRNA fractions, indicating that even relatively small quantities of linear RNA contaminants are able to induce a substantial cellular immune response in A549 cells. Late circRNA fractions elicited no cytokine response in excess of that from untransfected controls. Consistent with cytokine release observations, A549 cell viability 36 h post-transfection was significantly greater for late circRNA fractions compared to all of the other fractions (Figure 2D).

Because it was previously reported that circRNA may induce RIG-I transcription in a self-regulatory feedback loop (Chen et al., 2017), we analyzed RIG-I and IFN-β1 transcript induction upon transfection of A549 cells with late circRNA HPLC fractions. We observed a significantly weaker induction of both RIG-I and IFN-β1 transcripts for late circRNA fractions in comparison with precursor RNA and unpurified splicing reactions (Figure 2E). Furthermore, we found that RNase R treatment of splicing reactions alone was not sufficient to ablate this effect (Figure 2F), while contamination of purified circRNA with very small quantities of the RIG-I ligand 3p-hpRNA induced substantial RIG-I transcription (Figure S2D). In HeLa cells, transfection of RNase R-digested splicing reactions, but not purified circRNA, induced RIG-I and IFN-β1, although we found HeLa cells to be less sensitive than A549 cells to contaminating RNA species (Figure S2E). A time course experiment monitoring RIG-I, IFN-β1, IL-6, and RANTES transcript induction within the first 8 h after transfection of A549 cells with splicing reactions or fully purified circRNA did not reveal a transient response to circRNA (Figure S2F). Purified circRNA similarly failed to induce pro-inflammatory transcripts in RAW264.7 murine macrophages (Figure S2G). To generalize these findings to another synthetic circRNA construct, we tested the induction of pro-inflammatory transcripts in response to the transfection of A549 cells with purified circRNA containing an encephalomyocarditis virus (EMCV) internal ribosomal entry site (IRES) and EGFP coding region, and again failed to observe substantial induction (Figure S2H). These data demonstrate that non-circular components of the splicing reaction are responsible for the immunogenicity observed in previous studies and that circRNA is not a natural ligand for RIG-I.

Nucleoside Modification of circRNA Is Disruptive

Nucleoside modifications such as 5-methylcytidine (m5C) and ψ have been reported to decrease the immunogenicity of linear mRNA *in vitro* and in some contexts *in vivo* by preventing ribonucleotides from interacting with cellular RNA sensors such as the endosomal TLRs 3, 7, and 8 and RIG-I (Karikó et al., 2005; Durbin et al., 2016). m6A has been reported to mediate internal ribosome entry and translation on linear RNAs and separately on endogenous circRNAs (Meyer et al., 2015; Yang et al., 2017). The effects of these modifications on the utility of mRNA *in vivo* may be variable, however, as ψ-mRNA delivered to the liver does not reduce immunogenicity or improve protein production (Kauffman et al., 2016). Recently, it was reported that incorporation of m1ψ diminishes mRNA immunogenicity and improves protein expression to a greater degree than incorporation of ψ (Andries et al., 2015; Svitkin et al., 2017). The effects of nucleoside modifications on exogenous circRNA translation efficiency and immunogenicity have not been tested. Because of previous difficulties with circRNA purification, the immunogenicity of purified circRNA relative to that of unmodified linear mRNA has also not been assessed. Therefore, we sought to evaluate the GLuc expression stability and cytokine release profile of purified unmodified and m1ψ-modified circRNA in comparison to unmodified and m1ψ-modified linear mRNA in A549 and 293 cells (Figure 3A).

Initial attempts to circularize m1ψ-circRNA using the PIE method were unsuccessful, as complete replacement of uridine with m1ψ in PIE construct precursors abolished ribozyme activity, while partial replacement dramatically reduced splicing efficiency (Figure 3B). We turned to an alternative method of circRNA preparation using T4 RNA ligase I and splint oligonucleotides designed to bring the ends of the precursor RNA into proximity for ligation (Figure S3A; Petkovic and Müller, 2015). Using optimized splint oligonucleotides and annealing conditions, we were able to obtain 40% circularization efficiency of the 1.5 kb precursor RNA (Figures S3B and S3C). Complete replacement of uridine with m1ψ did not impede circularization using this method and we were able to obtain modified circular products (Figure 3C).

Upon transfection of 293 and A549 cells with m1ψ-circRNA, we observed no protein expression, and thus we were unable to determine the stability of protein expression from modified circRNA (Figure 3D). Unmodified circRNA displayed enhanced expression stability in HEK293 and A549 cells compared to both unmodified and modified linear mRNA (Figures 3E and S3D). We found that unmodified linear mRNA provoked a greater cytokine response than unmodified circRNA in immunoresponsive A549 cells, despite capping, phosphatase treatment, and

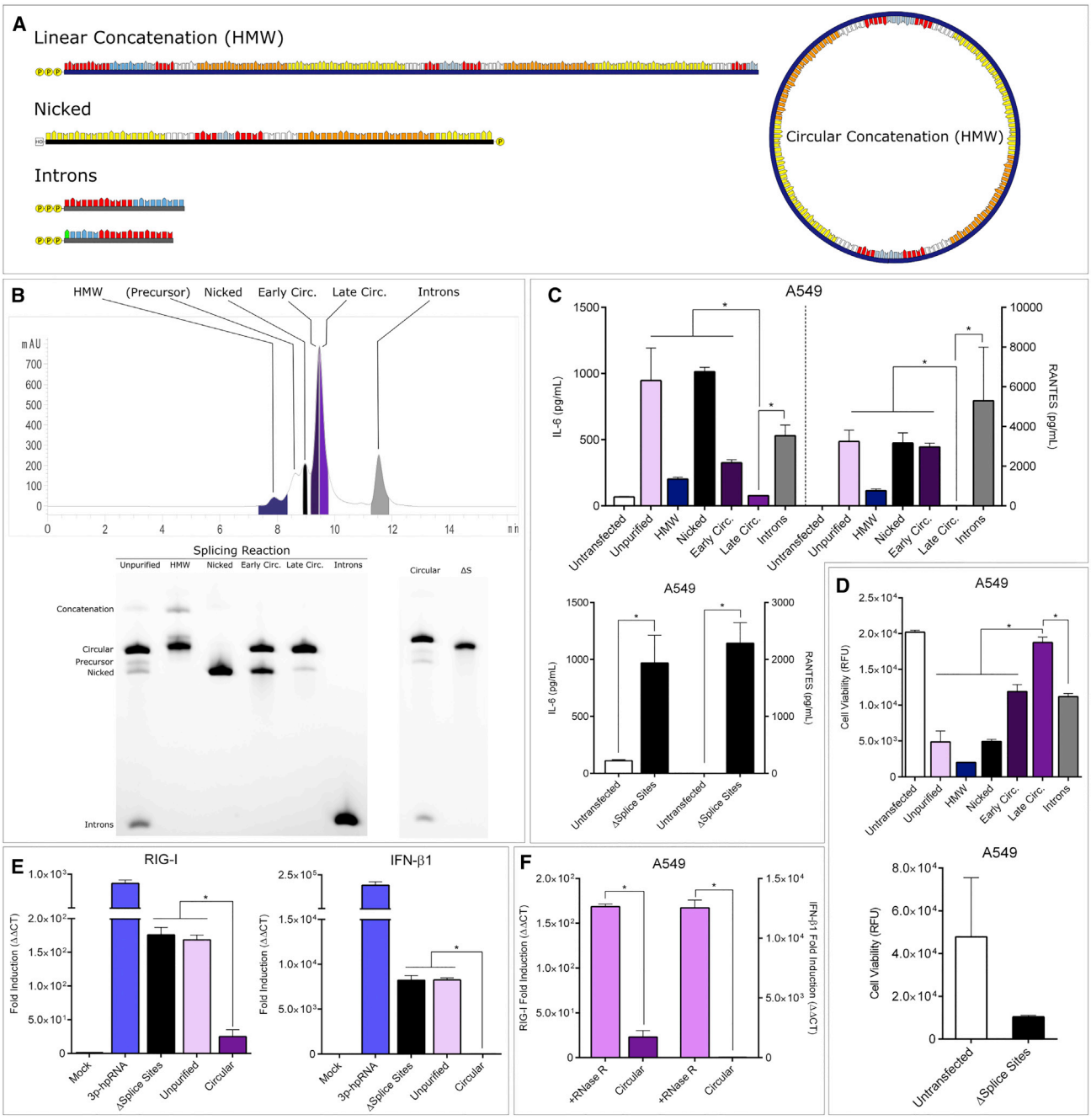

Figure 2. Splicing Reaction Fractionation and Assessment of Immunogenicity

(A) Schematics of RNAs introduced and used in this figure. HMW, high molecular weight; this fraction contains linear and circular concatenations.

(B) Top: HPLC chromatogram of an unpurified splicing reaction. Bottom: agarose gel of purified fractions. Adequate separation of precursor RNA was difficult, therefore, ΔS was used instead.

(C) Cytokine release 24 h after transfection of A549 cells with different HPLC fractions as described in (B) (data presented as means + SDs; n = 3; *p < 0.05).

(D) Cell viability 36 h after transfection of A549 cells with different HPLC fractions as described in (B) (data presented as means + SDs; n = 3; *p < 0.05).

(E) RIG-I and IFN-β1 transcript induction 18 h after transfection of A549 cells with the indicated RNAs. 3p-hpRNA is 5′ triphosphate hairpin RNA and a specific agonist of RIG-I (data presented as means + SDs; n = 3; *p < 0.05).

(F) RIG-I and IFN-β1 transcript induction 18 h after transfection of A549 cells with RNase R digested splicing reactions or the late circRNA fraction (data presented as means + SDs; n = 3; *p < 0.05).

See also Figure S2.

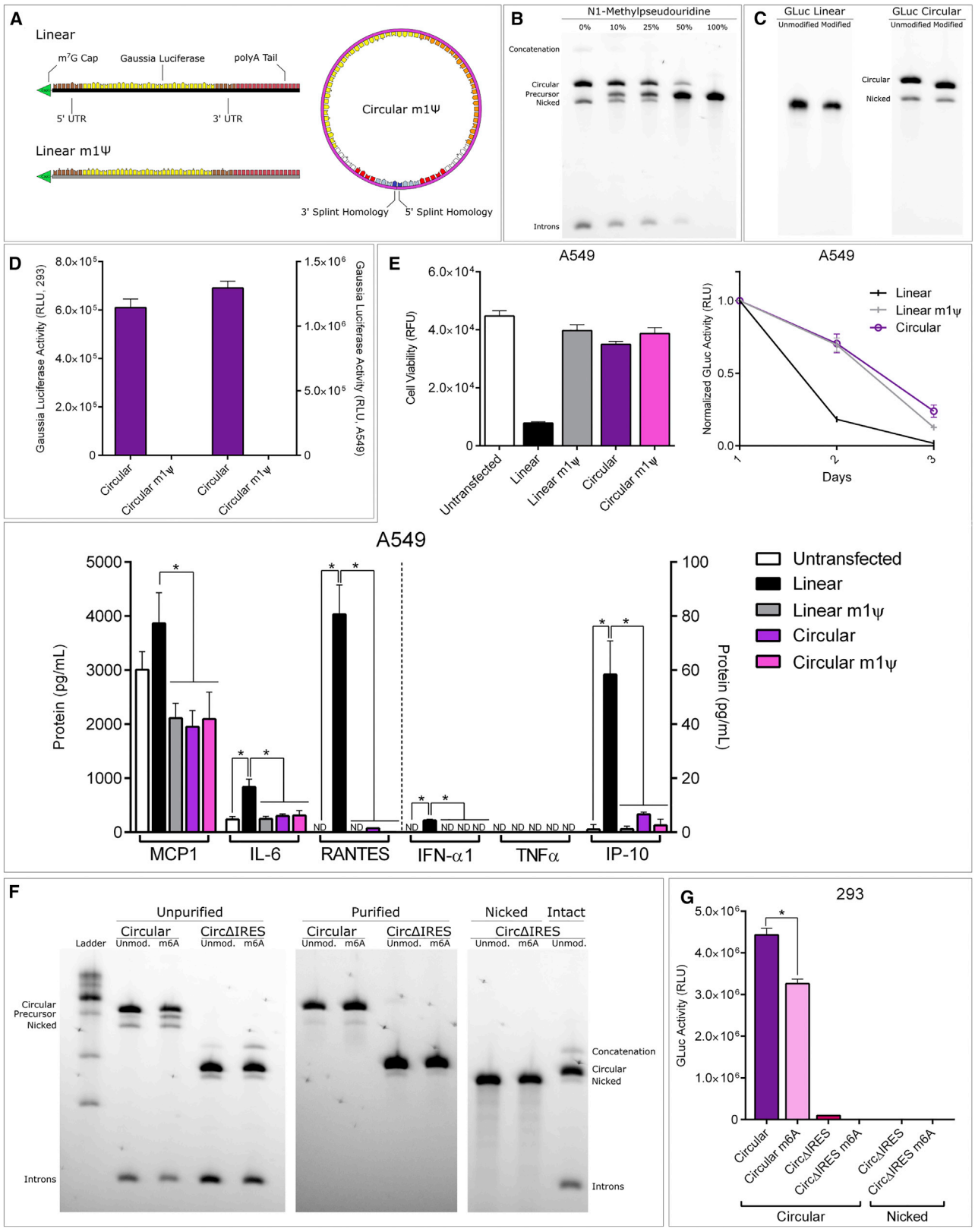

(legend on next page)

HPLC purification to remove RIG-I ligands. In contrast, both m1ψ-circRNA and m1ψ-mRNA did not significantly alter cytokine release profiles (Figures 3E and S3E). A549 cell viability was diminished upon the transfection of unmodified linear mRNA but not unmodified circRNA or either m1ψ-RNAs (Figure 3E). Consistent with data from Figure 1, we did not detect significant differences in 293 cytokine release at 24 h post-transfection and cell viability at 3 days post-transfection (Figures S3D and S3E). These experiments indicate that circRNA is less immunogenic than capped and polyadenylated linear mRNA and that nucleoside modification of circRNA is unnecessary for protection from innate immune sensors.

To test the effect of m6A on synthetic circRNA translation, we constructed a GLuc-coding circRNA with no IRES and an A-rich region upstream of the start codon (circΔIRES). A 10% replacement of adenosine with m6A reduced splicing of the longer circRNA construct containing the CVB3 IRES, but it did not affect the splicing of circΔIRES (Figure 3F). In 293 cells, protein expression from m6A-circRNA was significantly reduced compared to unmodified circRNA (Figure 3G). CircΔIRES modification with m6A failed to produce detectable levels of GLuc activity (Figure 3G). Site-specific nicking of m6A with oligonucleotide-guided RNase H upstream of the start codon, resulting in a linear RNA with an A-rich region followed by an intact GLuc coding sequence, did not rescue protein expression (Figures 3F and 3G). These data show that exogenous circRNA is unlikely to benefit from m6A modification and are consistent with previous reports indicating the involvement of nuclear RNA binding proteins in m6A-mediated translation (Lin et al., 2016).

circRNA Evades Detection by TLRs

Because capped and polyadenylated linear mRNAs were able to trigger cytokine secretion, while circRNA was not, we investigated the ability of different RNAs to activate TLRs in reporter cell lines. TLRs 3, 7, and 8 are known to detect RNA in endosomes and initiate an inflammatory cascade (Kawasaki and Kawai, 2014). TLR3 binds to dsRNA and stem structures in viral ssRNA (Tatematsu et al., 2013; Bell et al., 2006), while TLR7 and human TLR8 bind to ssRNA and nucleoside degradation products (guanosine for TLR7 and uridine for TLR8), with both ligands necessary for complete TLR activation (Tanji et al., 2015; Zhang et al., 2016). To control for structural and sequence differences between linear and circular RNAs, we constructed a linearized version of the circRNA. This construct contained all of the components of the spliced circRNA and was created by deleting the intron and homology arm sequences (linearized RNA; Figures 4A and S4A). All of the linearized RNAs were additionally treated with phosphatase (in the case of capped RNAs, after capping) and purified by HPLC. While we did not find a response to linearized or circular RNA in TLR7 reporter cells, both TLR3 and TLR8 reporter cells were activated by capped linearized RNA, polyadenylated linearized RNA, the nicked circRNA HPLC fraction, and the early circRNA fraction (Figure 4B). The late circRNA fraction did not provoke a TLR-mediated response in any cell line, similarly to m1ψ-mRNA (Figure 4B). However, the addition of uridine, but not cytidine, to the media of TLR8 reporter cells transfected with circRNA partially reverted this effect and resulted in secreted embryonic alkaline phosphatase (SEAP) secretion, indicating that *trans*-addition of one of the two RNA degradation signals needed for TLR8 activation can compensate for the lack of circRNA detection by TLR8 (Figures 4C and S4B).

Next, we linearized purified circRNA using two methods: treatment of circRNA with heat in the presence of magnesium ions and DNA oligonucleotide-guided RNase H digestion (Figure 4D). Both methods yielded a majority of full-length linear RNA with small amounts of intact circRNA, although heat treatment resulted in a greater proportion of lower-molecular-weight linear RNA degradation products (Figure 4E). Transfection of circRNA degraded by both heat and RNase H prompted SEAP secretion in TLR8 reporter cells (Figure 4F). No activation was observed in TLR3 and TLR7 reporter cells for degraded or intact conditions, despite the activation of TLR3 by *in vitro* transcribed linearized RNA (Figures 4F and S4C). These results indicate that circRNA is able to avoid detection by TLRs and that TLR8 evasion is a result of circular conformation.

Exogenous circRNA Is Translatable *In Vivo*

We next examined the translation and immunogenicity of unmodified and m1ψ-modified human erythropoietin (hEpo) linear mRNAs and circRNAs, with linear mRNAs identical to those depicted in Figure 3A, with the exception of the coding region (Figures S5A and S5F). Equimolar transfection of m1ψ-mRNA and unmodified circRNA resulted in robust protein expression in 293 cells (Figure S5B). hEpo linear mRNA and circRNA displayed similar relative protein expression patterns and cell viabilities in comparison to GLuc linear mRNA and circRNA upon equal weight transfection of 293 and A549 cells (Figures S5C and S5D). In mice, hEpo was detected in serum after the injection of hEpo circRNA or linear mRNA into visceral adipose (Figures 5A and 5D). hEpo detected after the injection of unmodified

Figure 3. Determination of circRNA Immunogenicity in Relation to Linear mRNA

(A) Schematics of RNAs introduced and used in this figure. Linear mRNAs do not contain an IRES or other structured features that may provoke a structure-specific immune response.

(B) Agarose gel showing progressive modification of circRNA precursor with m1ψ.

(C) Agarose gel showing purified unmodified and modified RNAs. Modification with m1ψ reduces apparent molecular weight.

(D) GLuc expression 24 h after transfection of 293 or A549 cells with unmodified circRNA or m1ψ-circRNA (data presented as means + SDs; n = 3).

(E) Cell viability, GLuc expression stability, and cytokine release from A549 cells transfected with unmodified or m1ψ linear mRNA or circRNA. Cell viability was assessed 3 days after transfection. Cytokine release was assessed 24 h after transfection (data presented as means + SDs; n = 3; $p < 0.05$; ns, not significant; ND, not detected).

(F) N^6-methyladenosine modification of circRNA. Left: agarose gel showing splicing products of unmodified and 10% m6A-modified circRNA with and without the CVB3 IRES. Center: agarose gel showing purified circRNAs. Right: agarose gel showing oligonucleotide-guided RNase H nicking of circΔIRES.

(G) GLuc expression 24 h after transfection of 293 cells with the indicated unmodified or m6A-modified RNAs (data presented as means + SDs; n = 3; $^*p < 0.05$). See also Figure S3.

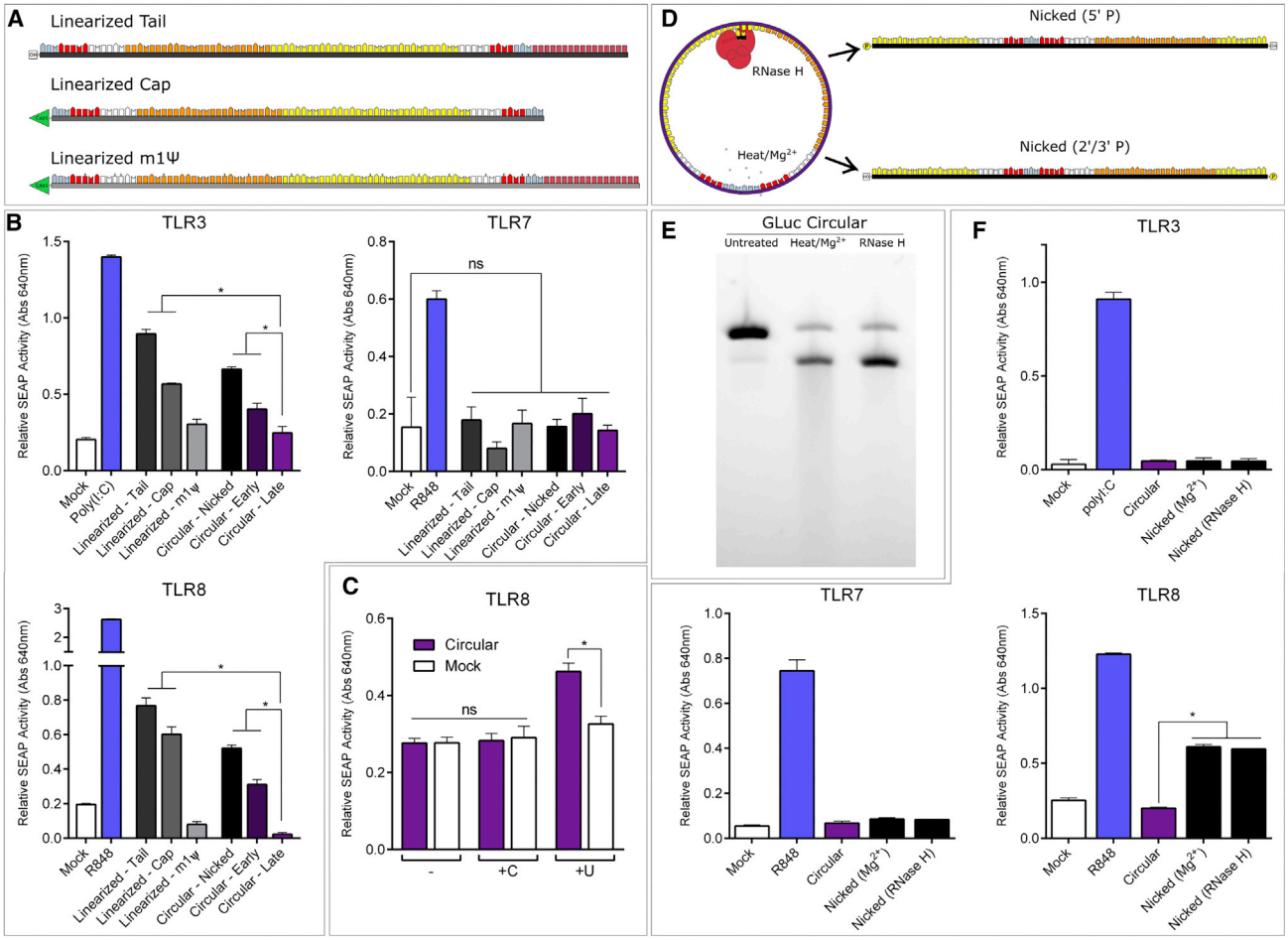

Figure 4. circRNA Evasion of TLRs

(A) Schematics of RNAs introduced and used for TLR experiments. Linearized circRNAs contain all of the same sequence elements as spliced circRNA due to deletions encompassing both the introns and the homology arms.

(B) SEAP expression 36 h after transfection of TLR reporter cells, with the indicated RNAs relative to null controls (data presented as means + SDs; n = 3; *p < 0.05; ns, not significant).

(C) SEAP expression 36 h after transfection of TLR8 reporter cells with the late circRNA fraction relative to the null control. −, media contains no nucleoside; C, media contains cytidine (3.5 mM); U, media contains uridine (3.5 mM). Data presented as means + SDs; n = 3; *p < 0.05; ns, not significant.

(D) Schematic of RNAs introduced and used for TLR nicked RNA experiments.

(E) Agarose gel showing alternative circRNA nicking strategies.

(F) SEAP expression 36 h after transfection of TLR reporter cells with the indicated RNAs relative to null controls (data presented as means + SDs; n = 3; *p < 0.05). See also Figure S4.

circRNA decayed more slowly than that from unmodified or m1ψ-mRNA and was still present 42 h post-injection (Figure 5B). We observed a rapid decline in serum hEpo upon the injection of unpurified circRNA splicing reactions or unmodified linear mRNA (Figure 5B). Injection of unpurified splicing reactions furthermore produced a cytokine response detectable in serum that we did not observe for the other RNAs, including purified circRNA (Figures 5C and S5E).

circRNA Is Compatible with Lipid Nanoparticles

Lipid nanoparticles have shown significant potential for use as delivery vehicles for therapeutic RNAs, including the delivery of mRNA to tissues (Oberli et al., 2017; Yanez Arteta et al., 2018; Kaczmarek et al., 2017). To assess the efficacy of lipid nanoparticles for circRNA delivery *in vivo*, we formulated purified circRNA into nanoparticles with the ionizable lipidoid cKK-E12 (Dong et al., 2014; Kauffman et al., 2015). These particles formed uniform multilamellar structures with an average size, polydispersity index, and encapsulation efficiency similar to that of particles containing commercially available control linear mRNA modified with 5moU (Figures 6A and S6A). Purified hEpo circRNA encapsulated in lipid nanoparticles (LNPs) displayed robust expression upon addition to 293 cells in comparison to 5moU-mRNA (Figure 6B, left). This commercially available 5moU-mRNA performed similarly to the m1ψ-mRNA we used previously (Figure S5B). Expression stability from LNP-RNA in

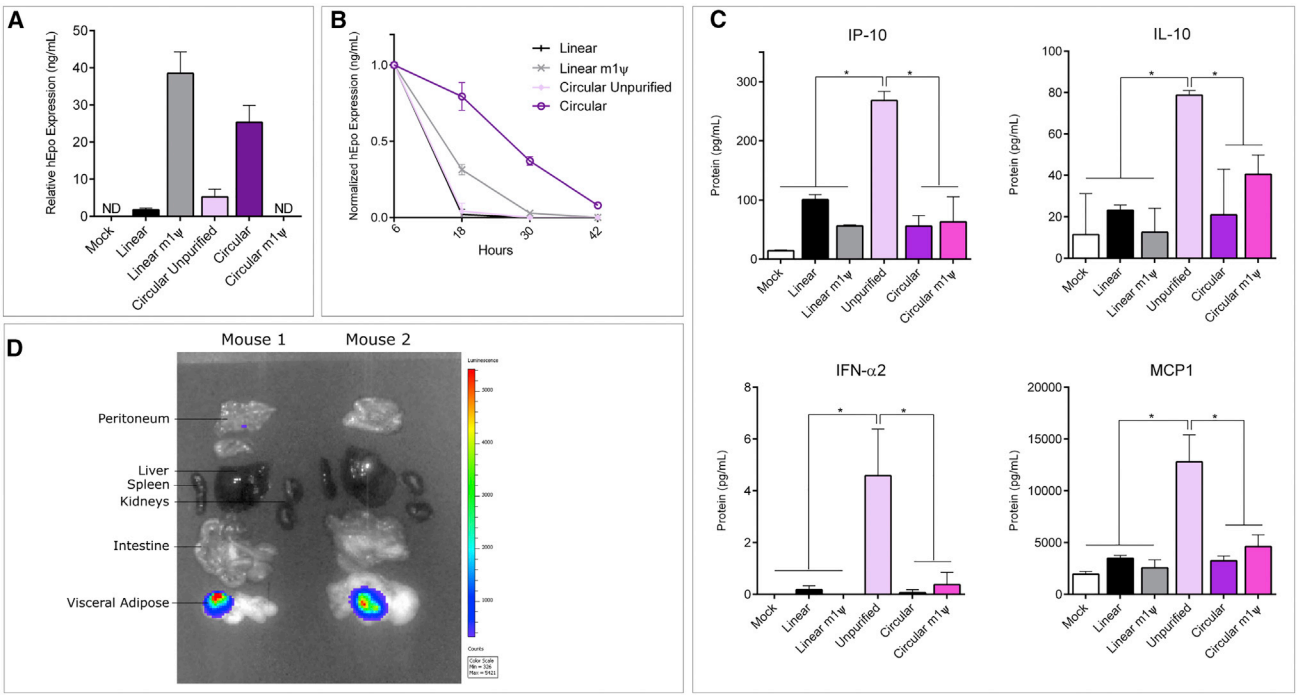

Figure 5. hEpo circRNA Characterization *In Vivo*

(A) Serum hEpo expression 6 h after injection of 350 ng unmodified or m1ψ linear mRNA or circRNA complexed with MessengerMax into visceral adipose tissue (data presented relative to molecular weight, means + SDs; n = 3).

(B) Relative hEpo expression in serum over 42 h (data presented as means + SDs; n = 3).

(C) Cytokines detected in serum 6 h after injection of 350 ng the indicated RNAs into visceral adipose (data presented as means + SDs; n = 3; *p < 0.05).

(D) Injection site demonstrated by injection of modified firefly luciferase mRNA complexed with MessengerMax.

See also Figure S5.

293 cells was similar to that from RNA delivered by transfection reagent, with the exception of a slight delay in decay for both 5moU-mRNA and circRNA (Figure 6B, right). Encapsulation in LNPs did not alter RIG-I/IFN-β1 induction or TLR activation *in vitro*, with unmodified circRNA failing to activate immune sensors in a manner similar to 5moU-mRNA (Figures 6C and 6D).

In mice, LNP-RNA was locally injected into visceral adipose tissue (Figure S6B). Serum hEpo expression from circRNA was lower but comparable with that from 5moU-mRNA 6 h after injection of LNP-RNAs into visceral adipose or intravenous delivery to liver (Figures 6E and S6E). Serum hEpo detected after adipose injection of unmodified LNP-circRNA decayed more slowly than that from LNP-5moU-mRNA, with a delay in expression decay present in serum that was similar to that noted *in vitro* (Figure 6F); however, serum hEpo detected after intravenous injection of LNP-circRNA decayed at almost the same rate as that from LNP-5moU-mRNA (Figure S6E). We did not observe an increase in serum cytokines or local RIG-I, TNF-α, or IL-6 transcript induction after the injection of LNP-5moU-mRNA or LNP-circRNA (Figure S6D).

DISCUSSION

In this work, we have demonstrated that exogenous circRNA evades RNA sensors and that the duration of protein expression is extended relative to linear mRNA following injection into mouse adipose tissue. While previous studies examining circRNA immunogenicity have proposed that exogenous circRNA provokes a strong innate cellular immune response mediated by RIG-I due to an absence of associated host splicing factors (Chen et al., 2017), we have found that exogenous circRNA does not activate several known cellular RNA sensors, including TLRs and RIG-I. These discordant results are likely to be the result of impurities in circRNA preparations. Previous studies have used circRNA purified by RNase R (Chen et al., 2017). We find that treatment with RNase R is not sufficient to obtain pure circRNA and enriches multiple resistant RNA species, which include circRNA and linear RNAs with structured 3′ ends. Furthermore, even small quantities of contaminating linear RNA, some of which may harbor triphosphates and may be present after HPLC purification, are sufficient to provoke robust cellular immune responses (Figure S2D). HPLC purification of circRNA presents unique difficulties, as nicked circRNA and intact circRNA are equal in molecular weight and their respective peaks partly overlap. Degradation products of triphosphorylated precursor RNA will also separate within the circRNA peak, and therefore gentle circRNA preparation is required. Phosphatase treatment, minimizing heat exposure in the presence of divalent cations, and stringent HPLC peak selection can reduce these hazards. Using the purification protocol described here, we

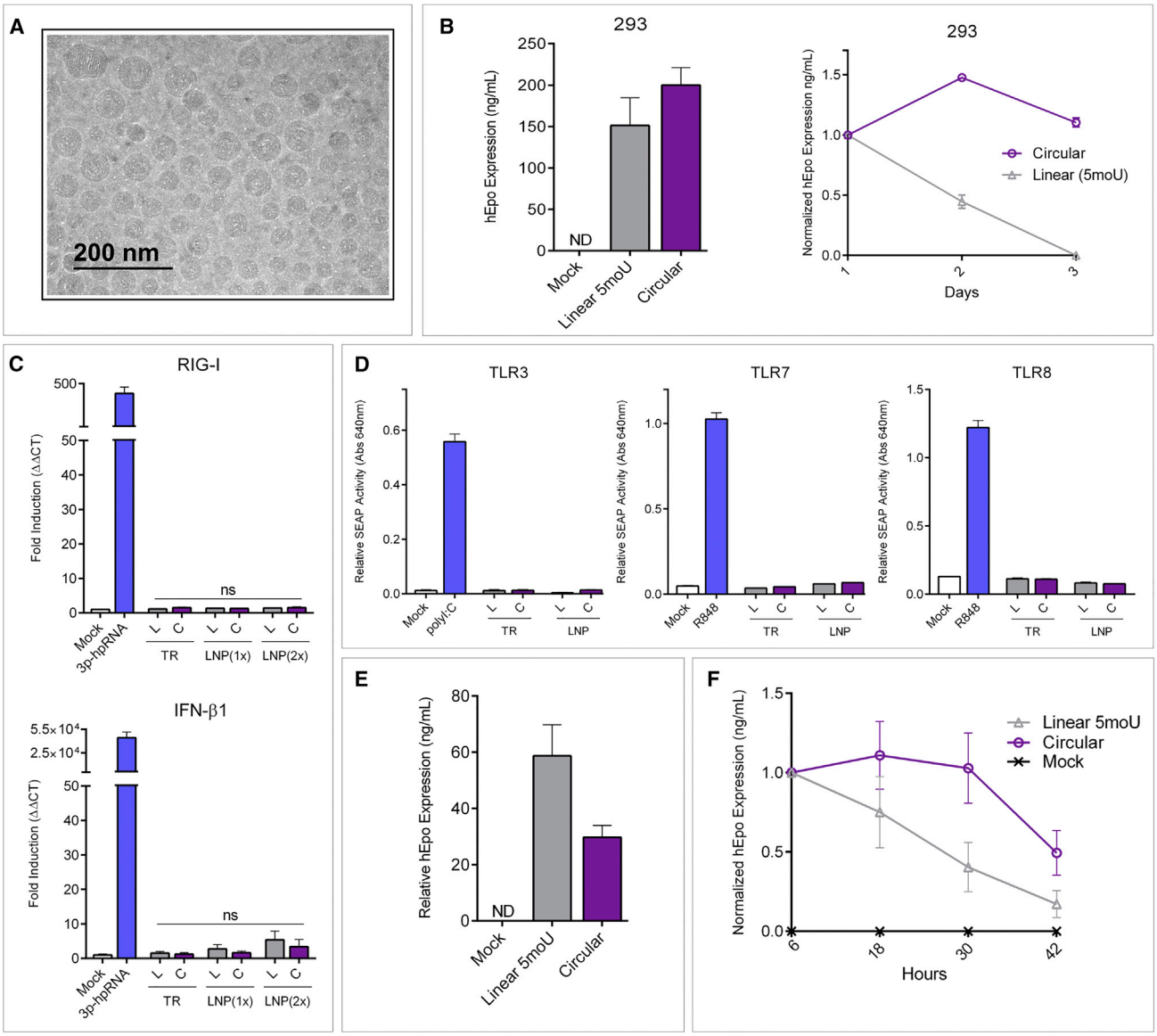

Figure 6. LNP-circRNA Characterization

(A) Cryogenic transmission electron microscopy (cryo-TEM) image of LNP-circRNA.

(B) hEpo expression 24 h after transfection of 293 cells with equimolar quantities of LNP-5moU-mRNA or unmodified LNP-circRNA (left) and hEpo expression stability over 3 days (right). Data presented as means + SDs; n = 3.

(C) RIG-I and IFN-β1 transcript induction 24 h after transfection of A549 cells with LNP-5moU-mRNA or unmodified LNP-circRNA. TR, transfection reagent plus 200 ng RNA (MessengerMax); LNP(1×), 200 ng LNP-RNA; LNP(2×), 400 ng LNP-RNA; L, 5moU-mRNA; C, circRNA. Data presented as means + SDs; n = 3; $p < 0.05$; ns, not significant).

(D) SEAP expression 48 h after transfection of TLR reporter cells with the RNAs indicated in (C), relative to null controls (data presented as means + SDs; n = 3).

(E) Serum hEpo expression 6 h after injection of 1.5 pmol LNP-5moU-mRNA or unmodified LNP-circRNA into visceral adipose (data presented as means + SDs; n = 5 linear 5moU, circular; n = 3 Mock).

(F) Relative hEpo expression in serum over 42 h after injection with LNP-RNAs (data presented as means + SDs; n = 5 linear 5moU, circular; n = 3 Mock).

See also Figure S6.

find that circRNA does not elicit substantial innate immune responses from TLR and RIG-I competent cells, in contrast to other components of the splicing reaction, or from mouse adipose tissue, despite the absence of circRNA-associated host splicing factors. In addition, protein expression from purified circRNA is significantly more stable than that from unpurified circRNA, and the transfection of purified circRNA results in greatly improved cell viability (Figures 1F and 2D), both of which are indicators of an antiviral response to non-circular contaminants in the unpurified conditions (Loo and Gale, 2011).

Nucleoside modifications, especially uridine modifications, have been reported to reduce linear mRNA immunogenicity by preventing detection by RNA sensors, which may be important for RNA function in some tissue types (Karikó et al., 2005; Durbin et al., 2016). With the constructs described here, we also observed enhanced protein expression stability from m1ψ-mRNA compared to unmodified mRNA *in vitro* and in adipose tissue (Figures 3E and 5B). This may be a secondary outcome of immune evasion or an unrelated primary effect of modification. Modification of RNA with m6A has been shown to promote cap-independent translation of endogenous linear and circular RNAs in living cells and exogenous linear RNAs in cell lysates (Meyer et al., 2015; Yang et al., 2017). We found that partial replacement of adenosine with m6A was not sufficient to drive translation from exogenous intact or linearized circRNA in living cells, consistent with previous reports indicating the involvement of nuclear RNA binding proteins in assisting m6A-dependent translation (Figures 3F and 3G; Lin et al., 2016).

Unlike linear mRNA, circRNA relies heavily on folded RNA structures, including the permuted group I intron and IRES, for splicing and translation. Modification of circRNA precursor molecules with m1ψ and m6A interfered with splicing in the PIE constructs and translation in the enzymatically circularized RNAs, suggesting that modifications significantly change the folding of these structural elements (Figures 3B, 3D, 3F, and 3G). The incorporation of ψ has been shown to enhance base-stacking interactions, which may lead to structural alterations (Davis, 1995); however, it is possible that other nucleoside modifications may be more compatible with ribozyme and IRES structures and allow for the study of modified circRNA stability during translation.

While it is known that modified linear mRNA is able to avoid detection by TLRs, we were surprised to discover that unmodified circRNA exhibits the same property (Figures 4 and S4). Recently, the ligands of TLR7 and TLR8 have been reported as degradation products of RNA, including short stretches of ssRNA and nucleosides (Tanji et al., 2015; Zhang et al., 2016). These degradation products are presumably produced by nucleases in the endosome shortly after the RNA is internalized (Roers et al., 2016). The contiguous structure of circRNA may confer it with resistance to endosomal nucleases, resulting in evasion of these detectors. In this case, endosomal nucleases would be expected to be composed primarily of exonucleases, as the presence of endonucleases would be expected to lead to circRNA degradation. Consistent with this postulation, the addition of one of the two cooperative TLR8 ligands, uridine, to the media of TLR8 reporter cells was able to partially abrogate the immunoevasive properties of circRNA, suggesting that a lack of degradation products, and therefore nuclease resistance, may indeed be responsible for TLR8 evasion by circRNA (Figure 4C). However, no degradation product has been defined as a ligand for TLR3, and circRNA also appears to evade it in the context of TLR3-overexpressing 293 cells, despite containing the same dsRNA motifs as the TLR3-activating linearized circRNA (Figure 4B). It may be possible that RNA degradation products bind to TLR3 at the dimerization interface in a similar manner to TLR8 (Roers et al., 2016). We furthermore observed differences in TLR3 activation by linearized circRNA, with *in vitro* transcribed linearized circRNA eliciting a TLR3-mediated response, while linearized circRNA produced by degrading purified circRNA did not (Figures 4B, 4F, and S4C). It is possible that the degradation of circRNA by either heat or RNase H disrupts the dsRNA structures that are required for robust TLR3 activation. Although we conducted functional assays in TLR-overexpressing cell lines, it may be possible that TLRs or other RNA sensors physically interact with circRNA, yet fail to activate a cellular immune response. Additional biochemical experiments exploring interactions between RNA sensors and circRNA are therefore warranted to fully elucidate the mechanism by which circRNA is able to evade detection.

Intra-adipose injection of circRNA complexed with transfection reagent or within LNPs yielded hEpo expression that was more stable than that from m1ψ-mRNA or 5moU-mRNA (Figures 5B and 6F). However, although we observed hEpo production from circRNA to be close to 2-fold higher than that from equimolar transfection of m1ψ-mRNA or 5moU-mRNA in 293 cells at 24 h, hEpo expression from circRNA *in vivo* was relatively diminished (Figures 5A and S5B). Several factors may have led to this result. The CVB3 IRES was originally selected for use in circRNA based on its ability to drive translation in human cell lines (Wesselhoeft et al., 2018). Mouse adipose or liver tissue may therefore not be the ideal cell type for CVB3 IRES-mediated translation. IRES sequences must also compete for translation initiation factors with endogenous transcripts bearing m^7G caps. Accordingly, circRNA using viral IRES sequences to initiate translation could be more effective in cells with higher initiation factor density relative to transcript density. A comprehensive characterization of the ability of other IRES sequences to drive translation from circRNA in diverse tissues is needed.

Protein expression stability from circRNA delivered intravenously by LNP to liver was not enhanced compared to that from 5moU-mRNA, although the relative magnitude of expression from circRNA at 6 h was comparable to that obtained from adipose tissue (Figures 6E and S6E). This result highlights tissue-specific stability that may be dependent on several factors, including general RNA turnover rate or endonuclease activity, sequence-specific translation inhibition or degradation, and the presence or absence of RNA stabilizing proteins. The assessment and alteration of microRNA (miRNA) binding sites within circRNA or the depletion of sequence-specific degradation motifs may further enhance circRNA stability and expression in select tissues.

We detected an increase in serum cytokines in mice injected with unpurified splicing reactions, but we did not detect a such a response in mice injected with unmodified mRNA, m1ψ-mRNA/5moU-mRNA, or circRNA (Figure 5C). Consistent with *in vitro* results, we observed a rapid decrease in hEpo expression upon injection of unmodified mRNA and unpurified splicing reactions, while serum hEpo after the injection of m1ψ-mRNA/5moU-mRNA and circRNA remained relatively stable, indicating that m1ψ-mRNA/5moU-mRNA and circRNA did not provoke a substantial immune response that would lead to RNA degradation *in vivo* (Figure 5B). The formulation of circRNA into LNPs did not alter immune sensor interactions, and analysis of serum cytokines and local pro-inflammatory transcript levels after LNP-RNA injections did not reveal an immune response against LNP-delivered circRNA (Figures 6C, 6D, and S6D).

We believe that the enhanced expression stability of circRNA in some tissues and the ability of circRNA to avoid immune sensors without the need for nucleoside modifications demonstrates the potential of circRNA as a vector for the expression of therapeutic proteins.

STAR★METHODS

Detailed methods are provided in the online version of this paper and include the following:

- KEY RESOURCES TABLE
- CONTACT FOR REAGENT AND RESOURCE SHARING
- EXPERIMENTAL MODEL AND SUBJECT DETAILS
  - Cell Lines
  - Animal Experiments
- METHOD DETAILS
  - RNA Design, Synthesis, and Purification
  - Splint Ligation
  - RNase H Nicking
  - Transfections and Cell Viability
  - Protein Expression Analysis
  - Reverse Transcription and qPCR
  - Lipid Nanoparticle Formulation
  - CRYO-TEM
  - ^{32}P-circRNA Assay
- QUANTIFICATION AND STATISTICAL ANALYSIS

SUPPLEMENTAL INFORMATION

Supplemental Information can be found with this article online at https://doi.org/10.1016/j.molcel.2019.02.015.

ACKNOWLEDGMENTS

This work was supported by the NIH (5R01HL125428), the Koch Institute Support (core) Grant from the National Cancer Institute (P30-CA14051), and the MIT School of Science Fellowship in Cancer Research. P.S.K. acknowledges funding from the Juvenile Diabetes Research Foundation (JDRF) postdoctoral fellowship (3-PDF-2017-383-A-N). We also thank the Nanotechnology Materials Core, the Animal Imaging and Preclinical Testing Core, and the Biopolymers and Proteomics Core Facilities at the MIT Koch Institute.

AUTHOR CONTRIBUTIONS

R.A.W., P.S.K., and N.B. conducted the experiments. R.A.W. wrote the manuscript. Y.H. and F.C.P.-H. assisted with the experiments. D.G.A. wrote the manuscript and provided guidance.

DECLARATION OF INTERESTS

R.A.W., P.S.K., and D.G.A. have filed a patent for the circRNA technology.

Received: October 8, 2018
Revised: December 13, 2018
Accepted: February 11, 2019
Published: March 19, 2019

REFERENCES

Andries, O., McCafferty, S., De Smedt, S.C., Weiss, R., Sanders, N.N., and Kitada, T. (2015). N(1)-methylpseudouridine-incorporated mRNA outperforms pseudouridine-incorporated mRNA by providing enhanced protein expression and reduced immunogenicity in mammalian cell lines and mice. J. Control. Release *217*, 337–344.

Barrett, S.P., and Salzman, J. (2016). Circular RNAs: analysis, expression and potential functions. Development *143*, 1838–1847.

Bell, J.K., Askins, J., Hall, P.R., Davies, D.R., and Segal, D.M. (2006). The dsRNA binding site of human Toll-like receptor 3. Proc. Natl. Acad. Sci. USA *103*, 8792–8797.

Chen, L.-L., and Yang, L. (2015). Regulation of circRNA biogenesis. RNA Biol. *12*, 381–388.

Chen, Y.G., Kim, M.V., Chen, X., Batista, P.J., Aoyama, S., Wilusz, J.E., Iwasaki, A., and Chang, H.Y. (2017). Sensing Self and Foreign Circular RNAs by Intron Identity. Mol. Cell *67*, 228–238.e5.

Davis, D.R. (1995). Stabilization of RNA stacking by pseudouridine. Nucleic Acids Res. *23*, 5020–5026.

Dong, Y., Love, K.T., Dorkin, J.R., Sirirungruang, S., Zhang, Y., Chen, D., Bogorad, R.L., Yin, H., Chen, Y., Vegas, A.J., et al. (2014). Lipopeptide nanoparticles for potent and selective siRNA delivery in rodents and nonhuman primates. Proc. Natl. Acad. Sci. USA *111*, 3955–3960.

Durbin, A.F., Wang, C., Marcotrigiano, J., and Gehrke, L. (2016). RNAs Containing Modified Nucleotides Fail To Trigger RIG-I Conformational Changes for Innate Immune Signaling. MBio. https://doi.org/10.1128/mBio.00833-16.

Hansen, T.B., Jensen, T.I., Clausen, B.H., Bramsen, J.B., Finsen, B., Damgaard, C.K., and Kjems, J. (2013). Natural RNA circles function as efficient microRNA sponges. Nature *495*, 384–388.

Hornung, V., Rothenfusser, S., Britsch, S., Krug, A., Jahrsdörfer, B., Giese, T., Endres, S., and Hartmann, G. (2002). Quantitative expression of toll-like receptor 1-10 mRNA in cellular subsets of human peripheral blood mononuclear cells and sensitivity to CpG oligodeoxynucleotides. J. Immunol. *168*, 4531–4537.

Jeck, W.R., and Sharpless, N.E. (2014). Detecting and characterizing circular RNAs. Nat. Biotechnol. *32*, 453–461.

Kaczmarek, J.C., Kowalski, P.S., and Anderson, D.G. (2017). Advances in the delivery of RNA therapeutics: from concept to clinical reality. Genome Med. *9*, 60.

Karikó, K., Buckstein, M., Ni, H., and Weissman, D. (2005). Suppression of RNA recognition by Toll-like receptors: the impact of nucleoside modification and the evolutionary origin of RNA. Immunity *23*, 165–175.

Karikó, K., Muramatsu, H., Welsh, F.A., Ludwig, J., Kato, H., Akira, S., and Weissman, D. (2008). Incorporation of Pseudouridine Into mRNA Yields Superior Nonimmunogenic Vector With Increased Translational Capacity and Biological Stability. Mol. Ther. *16*, 1833–1840.

Karikó, K., Muramatsu, H., Ludwig, J., and Weissman, D. (2011). Generating the optimal mRNA for therapy: HPLC purification eliminates immune activation and improves translation of nucleoside-modified, protein-encoding mRNA. Nucleic Acids Res. *39*, e142.

Kauffman, K.J., Dorkin, J.R., Yang, J.H., Heartlein, M.W., DeRosa, F., Mir, F.F., Fenton, O.S., and Anderson, D.G. (2015). Optimization of Lipid Nanoparticle Formulations for mRNA Delivery in Vivo with Fractional Factorial and Definitive Screening Designs. Nano Lett. *15*, 7300–7306.

Kauffman, K.J., Mir, F.F., Jhunjhunwala, S., Kaczmarek, J.C., Hurtado, J.E., Yang, J.H., Webber, M.J., Kowalski, P.S., Heartlein, M.W., DeRosa, F., and Anderson, D.G. (2016). Efficacy and immunogenicity of unmodified and pseudouridine-modified mRNA delivered systemically with lipid nanoparticles in vivo. Biomaterials *109*, 78–87.

Kawasaki, T., and Kawai, T. (2014). Toll-like receptor signaling pathways. Front. Immunol. *5*, 461.

Kos, A., Dijkema, R., Arnberg, A.C., van der Meide, P.H., and Schellekens, H. (1986). The hepatitis delta (delta) virus possesses a circular RNA. Nature *323*, 558–560.

Legnini, I., Di Timoteo, G., Rossi, F., Morlando, M., Briganti, F., Sthandier, O., Fatica, A., Santini, T., Andronache, A., Wade, M., et al. (2017). Circ-ZNF609 Is a Circular RNA that Can Be Translated and Functions in Myogenesis. Mol. Cell *66*, 22–37.e9.

Li, Z., Huang, C., Bao, C., Chen, L., Lin, M., Wang, X., Zhong, G., Yu, B., Hu, W., Dai, L., et al. (2015). Exon-intron circular RNAs regulate transcription in the nucleus. Nat. Struct. Mol. Biol. *22*, 256–264.

Lin, S., Choe, J., Du, P., Triboulet, R., and Gregory, R.I. (2016). The m(6)A Methyltransferase METTL3 Promotes Translation in Human Cancer Cells. Mol. Cell *62*, 335–345.

Loo, Y.-M., and Gale, M., Jr. (2011). Immune signaling by RIG-I-like receptors. Immunity *34*, 680–692.

Meyer, K.D., Patil, D.P., Zhou, J., Zinoviev, A., Skabkin, M.A., Elemento, O., Pestova, T.V., Qian, S.B., and Jaffrey, S.R. (2015). 5′ UTR m(6)A Promotes Cap-Independent Translation. Cell *163*, 999–1010.

Oberli, M.A., Reichmuth, A.M., Dorkin, J.R., Mitchell, M.J., Fenton, O.S., Jaklenec, A., Anderson, D.G., Langer, R., and Blankschtein, D. (2017). Lipid Nanoparticle Assisted mRNA Delivery for Potent Cancer Immunotherapy. Nano Lett. *17*, 1326–1335.

Petkovic, S., and Müller, S. (2015). RNA circularization strategies in vivo and in vitro. Nucleic Acids Res. *43*, 2454–2465.

Puttaraju, M., and Been, M.D. (1992). Group I permuted intron-exon (PIE) sequences self-splice to produce circular exons. Nucleic Acids Res. *20*, 5357–5364.

Roers, A., Hiller, B., and Hornung, V. (2016). Recognition of Endogenous Nucleic Acids by the Innate Immune System. Immunity *44*, 739–754.

Sanger, H.L., Klotz, G., Riesner, D., Gross, H.J., and Kleinschmidt, A.K. (1976). Viroids are single-stranded covalently closed circular RNA molecules existing as highly base-paired rod-like structures. Proc. Natl. Acad. Sci. USA *73*, 3852–3856.

Suzuki, H., Zuo, Y., Wang, J., Zhang, M.Q., Malhotra, A., and Mayeda, A. (2006). Characterization of RNase R-digested cellular RNA source that consists of lariat and circular RNAs from pre-mRNA splicing. Nucleic Acids Res. *34*, e63.

Svitkin, Y.V., Cheng, Y.M., Chakraborty, T., Presnyak, V., John, M., and Sonenberg, N. (2017). N1-methyl-pseudouridine in mRNA enhances translation through eIF2α-dependent and independent mechanisms by increasing ribosome density. Nucleic Acids Res. *45*, 6023–6036.

Tanji, H., Ohto, U., Shibata, T., Taoka, M., Yamauchi, Y., Isobe, T., Miyake, K., and Shimizu, T. (2015). Toll-like receptor 8 senses degradation products of single-stranded RNA. Nat. Struct. Mol. Biol. *22*, 109–115.

Tatematsu, M., Nishikawa, F., Seya, T., and Matsumoto, M. (2013). Toll-like receptor 3 recognizes incomplete stem structures in single-stranded viral RNA. Nat. Commun. *4*, 1833.

Wang, Y., and Wang, Z. (2015). Efficient backsplicing produces translatable circular mRNAs. RNA *21*, 172–179.

Wesselhoeft, R.A., Kowalski, P.S., and Anderson, D.G. (2018). Engineering circular RNA for potent and stable translation in eukaryotic cells. Nat. Commun. *9*, 2629.

Yanez Arteta, M., Kjellman, T., Bartesaghi, S., Wallin, S., Wu, X., Kvist, A.J., Dabkowska, A., Székely, N., Radulescu, A., Bergenholtz, J., and Lindfors, L. (2018). Successful reprogramming of cellular protein production through mRNA delivered by functionalized lipid nanoparticles. Proc. Natl. Acad. Sci. USA *115*, E3351–E3360.

Yang, Y., Fan, X., Mao, M., Song, X., Wu, P., Zhang, Y., Jin, Y., Yang, Y., Chen, L.L., Wang, Y., et al. (2017). Extensive translation of circular RNAs driven by N^6-methyladenosine. Cell Res. *27*, 626–641.

Zhang, Z., Ohto, U., Shibata, T., Krayukhina, E., Taoka, M., Yamauchi, Y., Tanji, H., Isobe, T., Uchiyama, S., Miyake, K., and Shimizu, T. (2016). Structural Analysis Reveals that Toll-like Receptor 7 Is a Dual Receptor for Guanosine and Single-Stranded RNA. Immunity *45*, 737–748.

STAR★METHODS

KEY RESOURCES TABLE

REAGENT or RESOURCE	SOURCE	IDENTIFIER
Chemicals, Peptides, and Recombinant Proteins		
RNase R	Applied Biological Materials	Cat#E049
3p-hpRNA	Invivogen	Cat#tlrl-hprna
polyI:C	Invivogen	Cat#tlrl-pic
RNase H	New England Biolabs	Cat#M0297S
T4 RNA Ligase 1	New England Biolabs	Cat#M0204S
Lipofectamine MessengerMAX Transfection Reagent	ThermoFisher Scientific	Cat#LMRNA003
N1-Methylpseudouridine-5′-Triphosphate	Trilink Biotechnologies	Cat#N-1081
CleanCap EPO mRNA (5moU)	Trilink Biotechnologies	Cat#L-7209
CleanCap FLuc mRNA (5moU)	Trilink Biotechnologies	Cat#L-7202
Alkaline Phosphatase, Calf Intestinal (CIP)	New England Biolabs	Cat#M0290S
Vaccinia Capping System	New England Biolabs	Cat#M2080S
mRNA Cap 2′-O-Methyltransferase	New England Biolabs	Cat#M0366S
E. coli Poly(A) Polymerase	New England Biolabs	Cat#M0276S
Uridine	Millipore Sigma	Cat#U6381
Cytidine	Millipore Sigma	Cat#C4654
1,2-dioleoyl-sn-glycero-3-phosphoethanolamine	Avanti Polar Lipids	Cat#850725P
1,2-dimyristoyl-sn-glycero-3-phosphoethanolamine-N-[methoxy-(polyethyleneglycol)-2000]	Avanti Polar Lipids	Cat#700100P
m6A-5′-Triphosphate	Trilink Biotechnologies	Cat#N-1013
Critical Commercial Assays		
E-Gel EX Agarose Gels, 2%	ThermoFisher Scientific	Cat# G401002
HiScribe T7 High Yield RNA Synthesis Kit	New England Biolabs	Cat#E2040S
MultiTox-Fluor Multiplex Cytotoxicity Assay	Promega	Cat#G9200
RNeasy Mini Kit	QIAGEN	Cat#74104
Human Erythropoietin Quantikine IVD ELISA Kit	R&D Systems	Cat#DEP00
BioLux Gaussia Luciferase Assay Kit	New England Biolabs	Cat#E3300
hCCL5 TaqMan Gene Expression Assay	ThermoFisher Scientific	Cat#Hs00982282m1
hIFNB1 TaqMan Gene Expression Assay	ThermoFisher Scientific	Cat#Hs01077958s1
hGAPDH TaqMan Gene Expression Assay	ThermoFisher Scientific	Cat#Hs99999905m1
hDDX58 TaqMan Gene Expression Assay	ThermoFisher Scientific	Cat#Hs01061436m1
hIL6 TaqMan Gene Expression Assay	ThermoFisher Scientific	Cat#Hs00714131m1
mCcl5 TaqMan Gene Expression Assay	ThermoFisher Scientific	Cat#Mm01302427m1
mIfnB1 TaqMan Gene Expression Assay	ThermoFisher Scientific	Cat#Mm00439552s1
mGapdh TaqMan Gene Expression Assay	ThermoFisher Scientific	Cat#Mm99999915 g1
mDdx58 TaqMan Gene Expression Assay	ThermoFisher Scientific	Cat#Mm01216853m1
mIl6 TaqMan Gene Expression Assay	ThermoFisher Scientific	Cat#Mm00446190m1
Tnf TaqMan Gene Expression Assay	ThermoFisher Scientific	Cat#Mm00443258_m1
Experimental Models: Cell Lines		
HEK-Blue Null1 Cells	Invivogen	Cat#hkb-null1
HEK-Blue Null2 cells	Invivogen	Cat#hkb-null2
HEK-Blue mTLR3	Invivogen	Cat#hkb-mtlr3
HEK-Blue mTLR7	Invivogen	Cat#hkb-mtlr7
HEK-Blue hTLR8	Invivogen	Cat#hkb-htlr8

(*Continued on next page*)

Continued		
REAGENT or RESOURCE	SOURCE	IDENTIFIER
293 [HEK293]	ATCC	Cat#CRL-1573
A549	ATCC	Cat#CCL-185
RAW264,7	ATCC	Cat#TIB-71
HeLa	ATCC	Cat#CCL-2
Experimental Models: Organisms/Strains		
C57BL/6 Mice	Charles River	Cat#C57BL/6NCrl
Oligonucleotides		
RNase H Probe: TTGAACCCAGGAATCTCAGG	This paper	N/A
Ligation Splint: GTTTGTGGTTCGTGCGTCTCCGTGCTGTTCTGTTGGTGTGGG	This paper	N/A
Recombinant DNA		
Plasmid: GLuc APIE CVB3 pAC	Wesselhoeft et al., 2018	N/A
Plasmid: hEpo APIE CVB3 pAC	Wesselhoeft et al., 2018	N/A
Plasmid: EGFP APIE EMCV	Wesselhoeft et al., 2018	N/A
Plasmid: GLuc APIE ΔIRES	This paper	N/A
Plasmid: GLuc APIE CVB3 pAC dS	Wesselhoeft et al., 2018	N/A
Plasmid: GLuc APIE CVB3 pAC dI	Wesselhoeft et al., 2018	N/A
Plasmid: splintGLuc CVB3	This paper	N/A
Plasmid: splinthEpo CVB3	This paper	N/A
Plasmid: GLuc L	This paper	N/A
Plasmid: hEpo L	This paper	N/A

CONTACT FOR REAGENT AND RESOURCE SHARING

Further information and requests for resources and reagents should be directed to and will be fulfilled by the Lead Contact, Daniel Anderson (dgander@mit.edu).

EXPERIMENTAL MODEL AND SUBJECT DETAILS

Cell Lines

293, A549, HeLa, and RAW264.7 cells (ATCC) and HEK-Blue mouse TLR3, mouse TLR7, human TLR8, Null1, and Null2 cells (Invivogen) were cultured at 37°C and 5% CO2 in Dulbecco's Modified Eagle's Medium (4500mg/L glucose) supplemented with 10% heat-inactivated fetal bovine serum (hiFBS, GIBCO) and penicillin/streptomycin. 293 and HeLa cells tested negative for mycoplasma. Cells were passaged every 2-3 days.

Animal Experiments

All animal experiments were performed under the guidelines of the MIT Animal Care and Use Committee. 30-35 g C57BL/6 female mice (Charles River) randomly assigned to treatment or control groups were injected into visceral fat through the lower right mammary fat pad and peritoneum with 350ng of RNA complexed with MessengerMax or 1.5 picomoles of LNP-RNA in a total volume of 50 μL, or intravenously by tail vein injection with 0.1mg/kg LNP-RNA. Blood samples were collected via tail bleed or cardiac puncture into BD Microtainer tubes at the indicated time points. To collect the serum, blood was allowed to coagulate for 15-30 min and was subsequently centrifuged at 2000xg for 5 min at room temperature. Human erythropoietin in 2uL of serum was detected as described previously. To collect adipose tissue, mice were sacrificed and the entire lower visceral adipose tissue was removed and frozen in liquid nitrogen for subsequent RNA isolation.

METHOD DETAILS

RNA Design, Synthesis, and Purification

Linear mRNA or circRNA precursors were synthesized by runoff in-vitro transcription from a linearized plasmid DNA template using a T7 High Yield RNA Synthesis Kit (New England Biolabs (NEB)) with the complete replacement of uridine with N^1-methylpseudouridine (Trilink Biotechnologies) for modified linear or circular RNA. After *in vitro* transcription, reactions were treated with DNase I (NEB) for 15 min. After DNase treatment, RNA was column purified using a MEGAclear Transcription Clean-up kit (Ambion). RNA was then heated to 70°C for 3 min and immediately placed on ice for 2 min, after which linear RNA was capped using mRNA

cap-2′-O-methyltransferase (NEB) and Vaccinia capping enzyme (NEB) according to the manufacturer's instructions. Polyadenosine tails were added to capped linear transcripts using *E. coli* PolyA Polymerase (NEB) according to manufacturer's instructions, and fully processed mRNA was column purified. For circRNA, GTP was added to a final concentration of 2mM along with a buffer including magnesium (50 mM Tris-HCl, 10 mM MgCl2, 1mM DTT, pH 7.5; NEB), and then reactions were heated at 55°C for 8 min. RNA was then column purified. In some cases, circRNA was digested with RNase R: 20μg of RNA was diluted in water (86uL final volume) and then heated at 70°C for 3 min and cooled on ice for 2 min. 20U RNase R and 10uL of 10x RNase R buffer (Applied Biological Materials) was added, and the reaction was incubated at 37°C for 15 min; an additional 10U RNase R was added halfway through the reaction. RNase R-digested RNA was column purified. In some cases, RNA was treated with a phosphatase (CIP, NEB): 20ug of RNA was diluted, heated and cooled as described above and then Cutsmart buffer (NEB) was added to a final concentration of 1X along with 20U of CIP. The reaction was incubated at 37°C for 15 min. Phosphatase-treated RNA was column purified. RNA was diluted in 50% formamide, denatured at 70°C for 3 min, and then cooled to room temperature. RNA was then separated on precast 2% E-gel EX agarose gels (Invitrogen) on the E-gel iBase (Invitrogen) using the E-gel EX 1%–2% program; ssRNA Ladder (NEB) was used as a standard. Bands were visualized using blue light transillumination and quantified using ImageJ. For high-performance liquid chromatography, 30μg of RNA was heated at 65°C for 3 min and then placed on ice for 2 min. RNA was run through a 4.6x300mm size-exclusion column with particle size of 5μm and pore size of 2000Å (Sepax Technologies; part number: 215980P-4630) on an Agilent 1100 Series HPLC (Agilent). RNA was run in RNase-free TE buffer (10mM Tris, 1mM EDTA, pH:6) at a flow rate of 0.3mL/minute. RNA was detected by UV absorbance at 260nm, but was collected without UV detection. Resulting RNA fractions were precipitated with 5M ammonium acetate, resuspended in water, and then in some cases subjected to further enzymatic treatment as described above. 5moU-modified Firefly Luciferase and hEpo mRNA was obtained from Trilink Biotechnologies.

Splint Ligation

Linear precursors for splint-mediated ligation were designed to have all of the same sequence features as PIE-circularized circRNA except for the addition of short adaptor sequences onto the 5′ and 3′ ends of the precursor RNA. These adaptor sequences shared homology with the splints used for circularization (Optimized splint: 5′-GTTTGTGGTTCGTGCGTCTCCGTGCTGTTCTGTT GGTGTGGG-3′). Splint ligation precursor RNA was synthesized as described previously, except a 10-fold excess of GMP was added to *in vitro* transcription reactions. 25ug of purified precursor RNA was heated to 70°C for 5 min in the presence of DNA splint at a concentration of 5uM in a 90uL reaction. The reaction was allowed to cool to room temperature, and then T4 RNA Ligase I Buffer (NEB) was added to a final concentration of 1X. ATP was added to a final concentration of 1mM. 50U of T4 RNA Ligase I (NEB) was added. Reactions were incubated at 37°C for 30 min and then column purified.

RNase H Nicking

Splicing reactions enriched for circRNA with RNase R and then column purified, or purified by HPLC, were heated at 70°C for 5 min in the presence of a DNA probe (5′-TTGAACCCAGGAATCTCAGG-3′) at five-fold molar excess, and then annealed at room temperature. Reactions were treated with RNase H (New England Biolabs) in the provided reaction buffer for 15 min at 37°C. RNA was column purified after digestion.

Transfections and Cell Viability

For 293 and A549 cells, 40ng of RNA was reverse transfected into 10,000 cells/100uL per well of a 96-well plate using Lipofectamine MessengerMax (Invitrogen) according to the manufacturer's instructions, unless otherwise noted. For HEK-Blue cells, 100ng of RNA was reverse transfected into 40,000 cells/100uL per well of a 96-well plate using Lipofectamine MessengerMax. For A549 cells transfected prior to RNA harvest and qPCR, 200ng of RNA was reverse transfected into 100,000 cells per well of a 24-well plate using Lipofectamine MessengerMax, unless otherwise noted. For experiments wherein protein expression was assessed at multiple time points, media was fully removed and replaced at each time point. For experiments wherein SEAP activity or cytokines were analyzed, media was not replaced between transfection and assessment. For all transfection experiments, RNA was heated to 70°C for 3 min and immediately placed on ice for 2 min prior to complexation with transfection reagent. Cell viability 36-72 h after transfection was assessed using a MultiTox kit (Promega). To detect SEAP secretion by TLR reporter and null cells, media was harvested 36-48 h after transfection and combined with HEK-Blue Detection reagent (Invivogen) to a final concentration of 1X. Media and detection reagent were incubated overnight at 37°C and then absorbance at 640nm was measured on an Infinite 200Pro Microplate Reader (Tecan). R848, polyI:C, and 3p-hpRNA were obtained from Invivogen. For TLR data in Figures 4 and 6, absorbance measured in TLR reporter cells was normalized to absorbance measured in null reporter cells containing only the plasmid with SEAP under the control of the IFN-β minimal promoter fused to five NF-κB and AP-1 binding sites for mTLR3 and hTLR8, or null reporter cells containing only the plasmid with SEAP under the control of the IL-12p40 minimal promoter fused to five NF-κB and AP-1 binding sites for mTLR7 (Invivogen).

Protein Expression Analysis

For luminescence assays, media was harvested 24 h post-transfection. To detect luminescence from Gaussia luciferase, 20uL of tissue culture medium was transferred to a flat-bottomed white-walled plate (Corning). 25uL of BioLux Gaussia Luciferase reagent including stabilizer (New England Biolabs) was added to each sample and luminescence was measured on an Infinite 200Pro

Microplate Reader (Tecan) after 45 s. Human erythropoietin was detected by solid phase sandwich ELISA (R&D Systems) essentially according to the manufacturer's instructions. Cytokines in Figures 1, 3, and 5 were detected by Fireplex immunoassay (Abcam). Cytokines in Figures 2 and 6 were detected by individual or multiplex immunoassay (Eve Technologies). For all multi-day GLuc and hEpo data, expression is presented relative to the first day of expression for each condition.

Reverse Transcription and qPCR

Cells were washed and RNA was harvested and purified 24 h after transfection using an RNeasy Mini Plus kit (QIAGEN) or RNeasy Lipid Kit (QIAGEN) for RNA extracted from mouse adipose tissue according to the manufacturer's instructions. Synthesis of first-strand cDNA from total RNA was performed with High-Capacity cDNA Reverse Transcription Kit using random hexamers (Thermo Fisher Scientific). Gene specific TaqMan primers were purchased as Assay-on-Demand (Thermo Fisher Scientific); human primers: GAPDH (Hs99999905_m1), DDX58 (Hs01061436_m1), IFN-β1 (Hs01077958_s1), CCL5 (Hs00982282_m1), IL-6 (Hs00714131_m1); mouse primers: Gapdh (Mm99999915_g1), Ddx58 (Mm01216853_m1), Il-6 (Mm00446190_m1), Tnf (Mm00443258_m1), Ifn-β1 (Mm00439552_s1), Ccl5 (Mm01302427_m1). The qPCR reaction was carried out using LightCycler 480 Probe Master Mix (Roche) and LightCycler 480 instrument (Roche). For each sample, threshold cycle values (Ct) were processed according to the comparative Ct method. Gene expression levels were normalized to the expression of the housekeeping gene GAPDH and presented relative to untransfected or mock transfection controls.

Lipid Nanoparticle Formulation

LNPs were prepared by mixing ethanol and aqueous phase at a 1:3 volumetric ratio in a microfluidic device, using syringe pumps as previously described. In brief, ethanol phase was prepared by solubilizing a mixture of ionizable lipidoid cKK-E12, 1,2-dioleoyl-sn-glycero-3-phosphoethanolamine (DOPE, Avanti), cholesterol (Sigma), and 1,2-dimyristoyl-sn-glycero-3-phosphoethanolamine-N-[methoxy-(polyethyleneglycol)-2000] (ammonium salt) (C14-PEG 2000, Avanti) at a molar ratio of 35:16:46.5:2.5. The aqueous phase was prepared in 10 mM citrate buffer (pH 3) with linear mRNA or circRNA. LNPs were dialyzed against PBS in a Slide-A-Lyzer G2 Dialysis Cassettes, 20,000 MWCO (Thermo Fisher) for 2h at RT. The concentration of mRNA encapsulated into LNPs nanoparticles was analyzed using Quant-iT RiboGreen assay (Thermo Fisher) according to the manufacturer's protocol. The efficiency of mRNA encapsulation into LNPs was calculated by comparing measurements in the absence and presence of 1% (v/v) Triton X-100. Nanoparticle size, polydispersity (PDI), and ζ-potential were analyzed by dynamic light scattering (DLS) using Zetasizer Nano ZS (Malvern Instruments, Worcestershire, UK). LNP hydrodynamic diameters are reported in the volume weighting mode and are an average of three independent measurements.

CRYO-TEM

For Cryogenic Transmission Electron Microscopy (Cryo-TEM) samples were prepared on a Gatan Cryo Plunge III (Cp3). Briefly, 3 uL of the sample was dropped on a lacey copper grid coated with a continuous carbon film and frozen in liquid ethane. Subsequently the frozen grid was mounted on a Gatan 626 single tilt cryo-holder. Imaging was performed using JEOL 2100 FEG microscope operating at 200 kV with a magnification of 10,000-60,000. All Images were recorded under low-dose conditions with a Gatan 2kx2k UltraScan CCD camera.

^{32}P-circRNA Assay

CircRNA precursor molecules were synthesized by *in vitro* transcription in the presence of 0.03mM α-^{32}P UTP. Radiolabeled RNA was spliced as described above and then circRNA was gel purified using a Zymoclean Gel RNA Recovery Kit (Zymo Research). 200ng of gel purified circRNA was transfected into 100,000 293 or A549 cells, and total RNA was harvested 6 and 24 h post transfection as described above. Purified total RNA was run on a 2% E-Gel EX agarose gel (Thermo Fisher) along with non-transfected radiolabeled unpurified and gel purified circRNA and ladder. The gel was placed onto filter paper and dried prior to exposure for 2 days, and then imaged using a Typhoon FLA 7000 scanner.

QUANTIFICATION AND STATISTICAL ANALYSIS

Statistical analysis of the results was performed by a two-tailed unpaired Welch's t test, assuming unequal variances. Differences were considered significant when $p < 0.05$. For all studies, data presented is representative of one independent experiment. Statistical details of individual experiments are present in figure legends.